



Title	Theoretical study of Ar-MCO (M = Pd, Pt)
Author(s)	Taketsugu, Yuriko; Noro, Takeshi; Taketsugu, Tetsuya
Citation	Chemical Physics Letters, 484(4-6), 139-143 https://doi.org/10.1016/j.cplett.2009.11.023
Issue Date	2010-01-07
Doc URL	https://hdl.handle.net/2115/42517
Type	journal article
File Information	CPL484-4-6_139-143.pdf



Theoretical study of Ar-MCO (M = Pd, Pt)

Yuriko Taketsugu ^a, Takeshi Noro ^b, Tetsuya Taketsugu ^{b,c,*}

^a Center for Strategic Utilization of Elements, Hokkaido University, Sapporo 060-0810, Japan

^b Division of Chemistry, Graduate School of Science, Hokkaido University, Sapporo 060-0810, Japan

^c Department of Theoretical and Computational Molecular Science, Institute for Molecular Science, Okazaki, 444-8585, Japan

Received 26 November 2008; in final form 29 October 2009

ABSTRACT

Ab initio calculations are performed for noble-gas complexes, Ar-PdCO and Ar-PtCO, by QCISD(T) with a Douglas-Kroll relativistic scheme. The electronic ground states of Ar-PdCO and Ar-PtCO are predicted to be $^1\Sigma$ with linear equilibrium structure, and the binding energy of Ar is estimated as 5.3 and 8.2 kcal/mol for Ar-PdCO and Ar-PtCO, respectively. The M-C-O (M = Pd, Pt) bending frequency in MCO increases by $\sim 10\%$ in Ar-MCO. The present calculations suggest that the experimentally reported M-C-O bending frequencies for MCO measured in the solid argon matrix are possibly to be assigned to the overtone band of the M-C-O bending mode of Ar-MCO.

* Corresponding author. Fax: +81-11-706-4921.
E-mail address: take@sci.hokudai.ac.jp (T.Taketsugu).

1. Introduction

Recent developments in *ab initio* electronic structure theory have made it possible to predict spectroscopic constants of weakly-bound complexes with high accuracy. The existence of super-strong van der Waals complexes containing noble-gas (Ng) atoms has been examined in both matrix-isolation spectroscopic experiments and theoretical calculations. For NiCO, for example, we reported theoretical calculations on Ar-NiCO [1] in which Ar is bound to NiCO with a binding energy of 9 kcal/mol. It was shown that the calculated bending frequency in NiCO increases by 10% due to the binding with Ar, resulting in good agreement with the corresponding experimental frequencies recorded for NiCO in solid argon [2]. Following our report [1], Tremblay and Manceron [3] reinvestigated vibrational spectra of NiCO in solid argon, neon, and mixed argon/neon matrices, and concluded that the species observed in solid argon should not be Ar-NiCO but NiCO. Then, we thoroughly reinvestigated [4] the structures, binding energies, and frequencies for NiCO and Ng-NiCO (Ng = He, Ne, Ar) by systematic theoretical calculations and suggested that Ne-NiCO and Ar-NiCO could be formed in the Ne- and Ar-matrix isolation experiments, respectively.

Pyykkö et al. [5] investigated a binding strength for the neutral species M-Xe (M = Ni, Pd, Pt) by *ab initio* methods with quasirelativistic pseudopotentials and reported that Pd-Xe and Pt-Xe were bound by 9.9 and 16.2 kcal/mol, respectively, while Ni-Xe has no bound states. Very recently, we investigated the stability of the possible noble-gas complexes of Ng-Pd-Ng' and Ng-Pt-Ng' (Ng, Ng' = Ar, Kr, Xe) by highly accurate *ab initio* calculations [6,7] and showed that two Ng atoms are bound with Pd or Pt atom in linear geometry due to $s-d_\sigma$ hybridization where the second Ng atom is bound to a metal with much larger energy than the first.

Since NiCO shows a relatively large binding energy with Ar, the binding strength for Ar-PdCO and Ar-PtCO deserves careful examination. In the present study, we have performed *ab initio* calculations for Ar-PdCO and Ar-PtCO with highest possible accuracy to determine their spectroscopic constants and binding energies. The results are discussed in comparison with the spectroscopic data for PdCO and PtCO determined by experiments in the gas phase and in argon matrix isolation.

2. Computational details

Ab initio electronic structure calculations were carried out to determine the equilibrium structures and harmonic frequencies for the ground state of Ar-PdCO and Ar-PtCO, as well as PdCO and PtCO, at the quadratic configuration interaction including singles and doubles with a perturbational estimate of triple excitations (QCISD(T)) level, using the MOLPRO program package [8]. In QCISD(T) calculations, the excitations from all valence orbitals of constituent atoms (for example, 5s and 4d for Pd, and 6s and 5d for Pt) were taken into account. Geometry optimizations and normal-mode analyses were performed for each complex under the assumption of linear geometry, by utilizing analytical energy gradients at the QCISD(T) level. Due to the restriction of the MOLPRO program, electronic structure calculations were performed under C_{2v} point group. We also performed geometry optimizations based on the counterpoise-corrected potential energy surface, to check effects of the basis set superposition error (BSSE) to the equilibrium geometry and the binding energy. The relativistic effects were included by using the 3rd-order Douglas-Kroll (DK3) relativistic scheme [9,10]. We used the relativistic basis sets developed by Tsuchiya et al. [11] for the inner and valence shells, which were split in valence parts of s and p functions and augmented by the correlated sets [12,13]. For PdCO and PtCO, we also carried out variational calculations to determine fundamental frequencies based on three-dimensional potential energy surface, using the RVIB3 code [14], where the potential energy surface was generated by fitting QCISD(T) energies at 252 points around the equilibrium structure to the 4th-order polynomials of the dimensionless Simons-Parr-Finlan stretching coordinates [15] and the M-C-O bending angle (M = Pd, Pt).

Since QCISD(T) is a single-reference-based method, we also performed complete active space multiconfigurational self-consistent field (CASSCF) calculations for the target molecules at their equilibrium structures to verify the applicability of QCISD(T). The active space for PdCO and Ar-PdCO includes 5s and 4d of Pd and all valence orbitals of C and O, while the active space for PtCO and Ar-PtCO includes 6s and 5d of Pt and all valence orbitals of C and O. As the results of CASSCF calculations, the CI coefficients for dominant electronic configuration are 0.956, 0.955, 0.955, and 0.956 for PdCO, Ar-PdCO, PtCO, and Ar-PtCO, respectively. The magnitude of these CI coefficients suggests that the present target molecules could be treated by a single-reference-based QCISD(T) approach.

3. Results and discussion

3.1. Structures and frequencies for PdCO and PtCO

Recently we reported a detailed ab initio study of spectroscopic constants for NiCO and Ng-NiCO (Ng = He, Ne, Ar) [4]. Since Ni, Pd, and Pt atoms belong to the same group in the periodic table, we first discuss geometries and vibrational frequencies for NiCO, PdCO, and PtCO. Table 1 shows calculated and experimental equilibrium bond lengths, harmonic frequencies, and fundamental frequencies for MCO (M = Ni, Pd, Pt), where experimental equilibrium bond lengths and frequencies from the rotational spectrum [16-20] are also given. These complexes are a linear molecule, and their ground-state term is $^1\Sigma$ [16,18,19]. The calculated M-C bond lengths are slightly shorter (by 0.001 ~ 0.007 Å), while the calculated CO bond lengths are slightly longer (by 0.004 ~ 0.010 Å) than the corresponding experimental values; the agreement between the theoretical calculations and the experiments is reasonable. In M-CO, σ -donation from CO to M and π -back-donation from M to CO π^* orbital determine the binding strength of M-C and C-O. Pd-CO shows the longest M-C bond length and the shortest C-O bond length among M-CO, indicating that Pd-CO has the weakest binding interaction between M and CO. For PdCO, preliminary non-relativistic calculations were also performed without a DK3 scheme and with non-relativistic basis-sets of almost the same quality as the relativistic ones, and the Pd-C bond distance was evaluated as 1.968 Å, which is 0.13 Å longer than the experimental value. This deviation indicates that an inclusion of the relativistic effect is crucial in theoretical calculations on PdCO and PtCO. Similar discussions for PdCO have been reported by Filatov [24]. We note for NiCO given in Table 1 that the NiC bond length calculated by non-relativistic calculations, 1.662 Å [9], is close to the experimental value, 1.669 Å [16].

The calculated harmonic frequencies for PdCO and PtCO agree well with the corresponding gas-phase experimental frequencies. We note that the gas-phase experimental harmonic frequencies are derived from the centrifugal distortion constants obtained from microwave spectra, and thus they may include errors of a few %. For PdCO, the Pd-C-O bending frequencies are 273 cm^{-1} (calc) and 270 cm^{-1} (gas phase exp), while Pd-C stretching frequencies are 479 cm^{-1} (calc) and 474 cm^{-1} (gas phase exp.). For PtCO, the Pt-C-O bending frequencies are 419 cm^{-1} (calc) and 420 cm^{-1} (gas phase exp),

while the Pt-C stretching frequencies are 605 cm^{-1} (calc) and 600 cm^{-1} (gas phase exp); thus the deviations in frequencies are only within 5 cm^{-1} .

Manceron et al. reported the fundamental frequencies measured by matrix isolation experiments for NiCO [2,3], PdCO [22], and PtCO [23]. Regarding the C-O and M-C stretching frequencies in PdCO and PtCO, good agreement between calculated and experimental values is observed. On the other hand, the M-C-O bending frequencies show large discrepancies in these complexes: 268 cm^{-1} (calc) vs. 616 cm^{-1} (Ar-matrix exp) in PdCO and 415 cm^{-1} (calc) vs. 917 cm^{-1} (Ar-matrix exp) in PtCO. The harmonic frequency for the Pd-C-O bending mode was evaluated by Filatov as 298 cm^{-1} at the MP4(SDQ) level; he suggested that the matrix-isolation experimental frequency (616 cm^{-1}) might be assigned to the overtone of the bending mode [24]. Similarly, Yamazaki et al. [20] pointed out that the matrix-isolation experimental frequency for the Pt-C-O bending mode (917 cm^{-1}) might be assigned to the overtone band based on their experimental frequency (420 cm^{-1}). They discussed that the Fermi resonance between the fundamental level of the Pt-C stretching mode and the overtone level of the Pt-C-O bending mode might introduce a relatively large intensity for the overtone band. In our variational calculations for vibrational eigenstates of PdCO and PtCO, however, we verified that there was no mixing between these two vibrational levels in both molecules. The overtone level of the Pd-C-O bending mode is calculated as 546 cm^{-1} for PdCO, while the overtone level of the Pt-C-O bending mode is calculated as 830 cm^{-1} for PtCO; thus they are both significantly smaller than the values observed in the matrix-isolation experiment. Note that the energy level of an overtone should be close to twice its fundamental frequency. We will return to this point in the next subsection.

3.2. Noble-gas complexes: *Ar-PdCO* and *Ar-PtCO*

Figure 1 shows the counterpoise-corrected QCISD(T) potential energy curves for Ar-MCO (M = Pd, Pt) as a function of $r(\text{Ar-M})$, where geometry of MCO is fixed to that of the isolated one. As is the case for Ar-NiCO investigated in Ref. [4], Ar atom is bound to both PdCO and PtCO with binding energies as high as 5 and 8 kcal/mol, respectively. Table 2 shows the atomic net charges from Mulliken population analyses at the QCISD level and the dipole moments at the QCISD(T) level for MCO and Ar-MCO (M = Pd, Pt). Both PdCO and PtCO have a dipole moment in the direction from the negatively charged O

atom to the positively charged metal atom. The dipole moment in Ar-MCO is larger than that in MCO due to a partial electron transfer from Ar to M. In Ar-MCO, the electrostatic attraction force due to a partial electron transfer should work to enhance the interaction between Ar and MCO from that expected from a dispersion force due to the induced dipole moments. This tendency is also seen in Ng-NiCO in our previous study [4].

Table 3 shows the equilibrium bond lengths and binding energies for MCO and Ar-MCO (M = Pd, Pt) by the QCISD(T) method. Through normal-mode analyses, all the complexes are shown to have a linear geometry as the minimum energy structure, with the ground-state term of $^1\Sigma$. Table 3 also shows the counterpoise (CP) corrected bond lengths and binding energies for Ar-MCO. The correction for BSSE works to enlarge M-C bond lengths by 0.013 ~ 0.014 Å and reduces the binding energy by 0.4 kcal/mol. The counterpoise-corrected binding energies between Ar and MCO (M = Pd, Pt) are evaluated as 5.28 and 8.17 kcal/mol for Ar-PdCO and Ar-PtCO, respectively.

Table 4 shows the harmonic frequencies, IR intensities, force constants, and reduced masses for normal modes of MCO and Ar-MCO (M = Pd, Pt) calculated by the QCISD(T) method. In both PdCO and PtCO, the binding with Ar atom introduces an increase in the M-C-O bending frequency by ~ 10% (from 273 to 315 cm^{-1} for Ar-PdCO and from 419 to 461 cm^{-1} for Ar-PtCO). The force constant for the M-C-O bending mode also increases from 0.57 to 0.75 $\text{mdyn}/\text{Å}$ (Ar-PdCO) and from 1.30 to 1.60 $\text{mdyn}/\text{Å}$ (Ar-PtCO), indicating that the curvature of the potential energy surface in the corresponding bending mode changes largely by the effect of Ar atom. In our previous studies [1,4], we showed that the Ni-C-O bending frequency in NiCO also increases by ~ 10% through binding with Ar or Ne atom and proposed that the vibrational spectra reported in the experiments of noble-gas matrix isolation for NiCO might be attributed to those of Ng-NiCO based on a relatively large binding energy between Ng and NiCO, as well as a good agreement in the calculated and experimental vibrational frequencies. Similarly, taking into account the binding energy between Ar and MCO (M = Pd, Pt), one can expect that the vibrational spectra measured in the experiments of argon matrix isolation for PdCO and PtCO are attributed to those of Ar-PdCO and Ar-PtCO, respectively. In the argon-matrix isolation experiments for PdCO and PtCO, the bending frequency was reported as 616 and 917 cm^{-1} , respectively. These numbers are very close to twice the fundamental frequency for the M-C-O bending mode calculated for Ar-MCO ($315 \times 2 = 630 \text{ cm}^{-1}$ for Ar-PdCO and $461 \times$

2 = 922 cm⁻¹ for Ar-PtCO), indicating that these experimental frequencies may be assigned to the overtone bands of Ar-PdCO and Ar-PtCO.

If the M-C-O bending fundamental frequencies of MCO (M = Pd, Pt) reported in the argon-matrix-isolation experiments were assigned to those of Ar-MCO, both C-O and M-C stretching fundamentals should also be assigned to those of Ar-MCO. As shown in Table 4, the C-O stretching harmonic frequency is scarcely affected by the binding with Ar, but the M-C stretching harmonic frequency changes by ~ 10 cm⁻¹ (479 to 491 cm⁻¹ for Ar-PdCO and 605 to 594 cm⁻¹ for Ar-PtCO). It is notable that the calculated and experimental M-C stretching fundamentals are 460 cm⁻¹ (calc) and 472 cm⁻¹ (Ar-matrix exp) for PdCO and 594 cm⁻¹ (calc) and 581 cm⁻¹ (Ar-matrix exp) for PtCO, as shown in Table 1. If the binding of Ar atom and the anharmonicity of the potential energy surface are both taken into account, the experimental M-C stretching fundamentals may be much closer to the fundamental frequencies for the M-C stretching modes of Ar-MCO than that of MCO.

We should also note that the IR intensity for the M-C-O bending mode decreases significantly in the Ar-MCO molecule (M = Pd, Pt). Especially in Ar-PtCO, the intensity of the fundamental band is calculated to change from 2.69 (PtCO) to 0.03 (Ar-PtCO). This indicates that, in the experimental vibrational spectra for Ar-MCO, the fundamental band of the M-C-O bending mode is too weak to be observable. As discussed in Sec. 3.1, the effect of Fermi resonance seems to be small in the overtone band of the M-C-O bending mode for both PdCO and PtCO. Although we have not calculated the vibrationally-excited energy levels for Ar-MCO because of the restriction of the program, we expect that the effect of Fermi resonance is so weak for Ar-PdCO and Ar-PtCO that the intensity of the overtone band of the M-C-O bending mode is still an open question. Ar-MCO has additional Ar-M stretching and Ar-MCO bending modes, but their weak intensities will hardly enable observation of the corresponding bands in the spectra.

We have also performed normal-mode analyses for isotopomers, ¹⁰⁶Pd¹³C¹⁶O, ¹⁰⁶Pd¹²C¹⁸O, ¹⁰⁶Pd¹³C¹⁸O, ¹⁹⁵Pt¹³C¹⁶O, ¹⁹⁵Pt¹²C¹⁸O, ¹⁹⁵Pt¹³C¹⁸O, and their complexes with ⁴⁰Ar atom at the QCISD(T) level. Variational calculations of fundamental frequencies were also performed for each complex based on the QCISD(T) potential energy surfaces. Table 5 shows harmonic and fundamental frequencies for the most abundant isotopomers of PdCO and PtCO (¹⁰⁶Pd¹²C¹⁶O and ¹⁹⁵Pt¹²C¹⁶O), harmonic frequencies for those of

Ar-PdCO and Ar-PtCO ($^{40}\text{Ar}-^{106}\text{Pd}^{12}\text{C}^{16}\text{O}$ and $^{40}\text{Ar}-^{195}\text{Pt}^{12}\text{C}^{16}\text{O}$), their isotopic shifts, and the corresponding experimental frequencies observed in a solid argon matrix [22,23]. The calculated isotopic shifts in the C-O and M-C stretching modes agree with their experimental values, whereas those in the M-C-O bending mode show large discrepancies. If the experimental M-C-O-bending frequencies are assigned to their overtone levels, the experimental isotopic shifts should be compared to twice the isotopic shifts for the fundamental frequencies. Twice the isotopic shifts for M-C-O bending vibration brings the calculated and experimental values into coincidence.

The comparison of these values indicates that the experimental frequencies for Pd-C-O and Pt-C-O bending modes should be assigned to the overtone band of Ar-PdCO and Ar-PtCO, respectively, and therefore, the vibrational spectra for PdCO and PtCO detected in the solid argon matrix may be attributed to those of new noble-gas complexes, Ar-PdCO and Ar-PtCO, respectively. A further spectroscopic examination is awaited.

4. Concluding remarks

We have examined the geometrical structures, binding energies, and vibrational frequencies for 1:1 complexes of Ar-MCO (i.e., Ar-PdCO and Ar-PtCO), as well as PdCO and PtCO, by the QCISD(T) method with the 3rd-order Douglas-Kroll relativistic scheme. The results have been discussed with reference to our recent report on Ar-NiCO. Being similar to the case of Ar-NiCO [1], the Ar atom can be bound to both PdCO and PtCO with strong van der Waals interaction energies (5.3 and 8.2 kcal/mol for Ar-PdCO and Ar-PtCO, respectively), which significantly exceed the normal van der Waals interaction energy expected for the complex of noble gas atoms and neutral molecules (< 1.0 kcal/mol). We have also verified that only one Ar atom is bound to MCO (M = Pd, Pt) with strong van der Waals interaction. These results provide us a picture that, once MCO is formed in the argon matrix, one Ar atom is promptly attached to MCO, resulting in Ar-MCO, being surrounded by solvent Ar atoms with much weaker interactions.

The results of our analyses suggest that the experimental bands for Ar-MCO (M = Pd, Pt) that had been assigned to the M-C-O bending fundamentals [22,23] are to be reassigned to the first overtone bands of the M-C-O bending mode. Correct assignments for these and other of Ng-MCO complexes will be provided by future spectroscopic experiments.

Acknowledgments

The present work was supported in part by a Grant-in-Aid for the Project on Strategic Utilization of Elements, and in part by a Grant-in-Aid for Scientific Research from the Ministry of Education, Culture, Sports, Science and Technology.

References

- [1] Y. Ono, T. Taketsugu, Chem. Phys. Lett. 385 (2004) 85.
- [2] H.A. Joly, L. Manceron, Chem. Phys. 226 (1998) 61.
- [3] B. Tremblay, L. Manceron, Chem. Phys. Lett. 429 (2006) 464.
- [4] Y. Taketsugu, T. Noro, T. Taketsugu, J. Phys. Chem. A 112 (2008) 1018.
- [5] J.V. Burda, N. Runeberg, P. Pyykkö, Chem. Phys. Lett. 288 (1998) 635.
- [6] Y. Ono, T. Taketsugu, T. Noro, J. Chem. Phys. 123 (2005) 204321.
- [7] Y. Taketsugu, T. Taketsugu, T. Noro, J. Chem. Phys. 125 (2006) 154308.
- [8] MOLPRO, version 2006.1, A Package of Ab Initio Programs, H.-J. Werner, P.J. Knowles, R. Lindh, F.R. Manby, M. Schutz et al., see <http://www.molpro.net>.
- [9] N. Douglas, N.M. Kroll, Ann. Phys. 82 (1974) 89.
- [10] B.A. Hess, Phys. Rev. A 33 (1986) 3742.
- [11] T. Tsuchiya, M. Abe, T. Nakajima, K. Hirao, J. Chem. Phys. 115 (2001) 4463.
- [12] T. Noro, M. Sekiya, T. Koga, Theor. Chem. Acc. 98 (1997) 25.
- [13] <http://setani.sci.hokudai.ac.jp/sapporo/>
- [14] S. Carter, N.C. Handy, Mol. Phys. 57 (1986) 175.
- [15] G. Simons, R.G. Parr, J.M. Finlan, J. Chem. Phys. 59 (1973) 3229.
- [16] E. Yamazaki, T. Okabayashi, M. Tanimoto, J. Am. Chem. Soc. 126 (2004) 1028.
- [17] T. Yamamoto, E. Okabayashi, T. Okabayashi, M. Tanimoto, The 1st Symposium of Japan Society for Molecular Science, Abstract 1P104, 2007.
- [18] N.R. Walker, J.K.-H. Hui, M.C.L. Gerry, J. Phys. Chem. A 106 (2002) 5803.
- [19] C.J. Evans, M.C.L. Gerry, J. Phys. Chem. A 105 (2001) 9659.
- [20] E. Yamazaki, T. Okabayashi, M. Tanimoto, Chem. Phys. Lett. 396 (2004) 150.
- [21] A. Martinez, M.D. Morse, J. Chem. Phys. 124 (2006) 124316.
- [22] B. Tremblay, L. Manceron, Chem. Phys. 250 (1999) 187.
- [23] L. Manceron, B. Tremblay, M.E. Alikhani, J. Phys. Chem. A 104 (2000) 3750.
- [24] M. Filatov, Chem. Phys. Lett. 373 (2003) 131.

Table 1

Calculated and experimental equilibrium bond lengths, harmonic frequencies, and fundamental frequencies (numbers in parentheses) for NiCO, PdCO, and PtCO.

Molecule (cm ⁻¹)	Method	Bond length (Å)		Frequency		
		$r(\text{M-C})$	$r(\text{C-O})$	$\nu(\text{CO})$	$\nu(\text{MCO})$	
					$\nu(\text{MC})$	
NiCO	CCSD(T) ^a	1.662	1.157	2034	375	618
	Exp (gas phase)	1.669 ^b	1.153 ^b	(2010.7) ^c	363 ^d	604 ^b
	Exp (Ar matrix) ^e			(1995)	(409)	(591)
	Exp (Ne matrix) ^f			(2007)	(399)	(593)
PdCO	QCISD(T)	1.835	1.146	2071	273	479
				(2040)	(268)	(460)
	Exp (gas phase) ^g Exp (Ar matrix) ^h	1.840 ^g	1.136 ^g	(2044)	270 ^d (616)	474 ^g (472)
PtCO	QCISD(T)	1.760	1.151	2081	419	605
				(2052)	(415)	(594)
	Exp (gas phase) Exp (Ar matrix) ^k	1.760 ⁱ	1.144 ⁱ	(2052)	420 ^j (917)	600 ^j (581)

^a Ref. [4].

^b Ref. [16].

^c Ref. [21].

^d Ref. [17].

^e Ref. [2].

^f Ref. [3].

^g Ref. [18].

^h Ref. [22].

ⁱ Ref. [19].

^j Ref. [20].

^k Ref. [23].

Table 2

QCISD Mulliken atomic charges q and QCISD(T) dipole moments μ (in Debye) for MCO and Ar-MCO (M = Pd, Pt).

	$q(\text{M})$	$q(\text{C})$	$q(\text{O})$	$q(\text{Ar})$	μ
PdCO	0.243	-0.144	-0.099		2.62
Ar-PdCO	0.173	-0.090	-0.117	0.034	3.27
PtCO	0.156	-0.005	-0.151		2.52
Ar-PtCO	0.014	0.082	-0.165	0.069	3.72

Table 3

Bond lengths (Å) and binding energy (kcal/mol) for MCO and Ar-MCO (M = Pd, Pt), calculated by QCISD(T).

	Bond length			Binding energy
	$r(\text{M-C})$	$r(\text{C-O})$	$r(\text{Ar-M})$	
PdCO	1.835	1.146		
Ar-PdCO	1.833	1.146	2.542	5.70
CP-corrected	1.834	1.146	2.555	5.28
PtCO	1.760	1.151		
Ar-PtCO	1.776	1.151	2.495	8.57
CP-corrected	1.774	1.151	2.509	8.17

Table 4

Harmonic frequencies (cm^{-1}), IR intensities (km mol^{-1}), force constants (mdyn \AA^{-1}), and reduced masses (amu) for the respective vibrational modes of MCO and Ar-MCO (M = Pd, Pt) calculated by QCISD(T).

Frequency	$\nu(\text{CO})$	$\nu(\text{MCO})$	$\nu(\text{MC})$	$\nu(\text{ArM})$	$\nu(\text{ArMCO})$
PdCO					
Frequency	2071	273	479		
Intensity	626.38	6.90	18.85		
Force Constant	33.67	0.57	2.35		
Reduced Mass	13.32	12.86	17.31		
Ar-PdCO					
Frequency	2073	315	491	142	50
Intensity	765.03	3.15	28.44	0.00	0.16
Force Constant	33.73	0.75	2.48	0.48	0.04
Reduced Mass	13.32	12.89	17.39	40.54	29.06
PtCO					
Frequency	2081	419	605		
Intensity	587.56	2.69	6.41		
Force Constant	33.81	1.30	3.49		
Reduced Mass	13.19	12.78	16.22		
Ar-PtCO					
Frequency	2087	461	594	170	70
Intensity	791.08	0.03	15.29	0.15	0.00
Force Constant	33.90	1.60	3.34	0.75	0.08
Reduced Mass	13.20	12.76	16.08	43.87	26.17

Table 5

Calculated and matrix-isolation experimental frequencies and isotopic shifts (in cm^{-1}) for isotopomers of MCO and Ar-MCO (M = Pd, Pt).

		Frequency (cm^{-1})			Isotopic shift (cm^{-1})								
		Pd ¹² C ¹⁶ O	ArPd ¹² C ¹⁶ O	Exp. ^{a)}	Pd ¹³ C ¹⁶ O	ArPd ¹³ C ¹⁶ O	Exp. ^{a)}	Pd ¹² C ¹⁸ O	ArPd ¹² C ¹⁸ O	Exp. ^{a)}	Pd ¹³ C ¹⁸ O	ArPd ¹³ C ¹⁸ O	Exp. ^{a)}
		Pt ¹² C ¹⁶ O	ArPt ¹² C ¹⁶ O	Exp. ^{b)}	Pt ¹³ C ¹⁶ O	ArPt ¹³ C ¹⁶ O	Exp. ^{b)}	Pt ¹² C ¹⁸ O	ArPt ¹² C ¹⁸ O	Exp. ^{b)}	Pt ¹³ C ¹⁸ O	ArPt ¹³ C ¹⁸ O	Exp. ^{b)}
$\nu(\text{CO})$	Harmonic	2070.9	2072.7	-	-48.9	-49.0	-	-45.9	-45.7	-	-96.1	-96.1	-
	Fundamental	2040.0	-	2044.2	-47.4	-	-47.4	-44.6	-	-44.7	-93.3	-	-93.5
$\nu(\text{PdCO})$	Harmonic	272.7	314.9	-	-8.2	-9.8	-	-3.4	-3.2	-	-11.7	-13.1	-
	Fundamental	268.2	-	615.7	-8.0	-	-19.0	-3.2	-	-6.0	-11.3	-	-25.3
$\nu(\text{PdC})$	Harmonic	478.7	491.1	-	-6.0	-6.1	-	-13.8	-14.1	-	-19.1	-19.5	-
	Fundamental	459.5	-	472.1	-5.8	-	-5.6	-12.9	-	-13.4	-18.0	-	-18.3
$\nu(\text{CO})$	Harmonic	2081.0	2086.6	-	-52.0	-52.0	-	-41.5	-42.1	-	-95.1	-95.5	-
	Fundamental	2051.7	-	2051.9	-50.6	-	-50.1	-40.5	-	-41.1	-92.5	-	-92.8
$\nu(\text{PtCO})$	Harmonic	419.3	460.8	-	-12.8	-14.7	-	-5.0	-4.4	-	-18.0	-19.2	-
	Fundamental	414.5	-	916.8	-12.6	-	-28.8	-4.9	-	-8.4	-17.6	-	-
$\nu(\text{PtC})$	Harmonic	605.4	593.6	-	-7.5	-7.6	-	-20.4	-20.1	-	-27.0	-26.7	-
	Fundamental	594.3	-	580.8	-7.1	-	-7.4	-20.1	-	-19.0	-26.2	-	-25.7

^a Ref. [22].

^b Ref. [23].

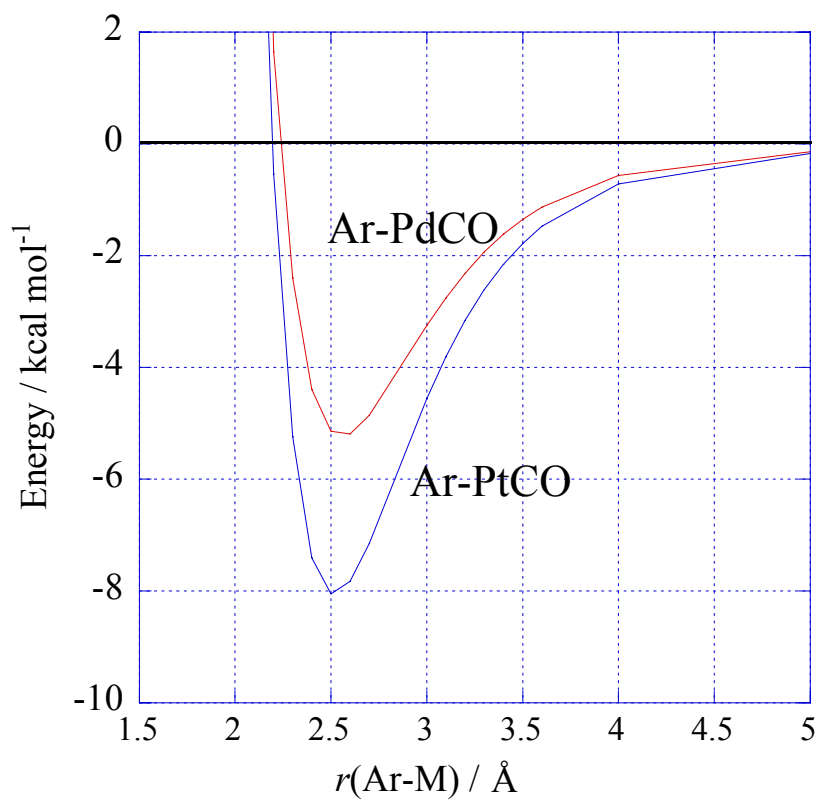


Fig. 1. Counterpoise corrected QCISD(T) potential energy curves for Ar-MCO (M = Pd, Pt).